Geophysical Research Letters

RESEARCH LETTER
10.1029/2018GL079677

Key Points:
- A strongly coupled data assimilation system is developed for tropical cyclone forecast
- Synthetic coastal surface currents are assimilated
- The intensity forecast is significantly improved

Supporting Information:
- Supporting Information S1

Correspondence to:
Y. Li,
y.li14@imperial.ac.uk

Citation:
Li, Y., & Toumi, R. (2018). Improved tropical cyclone intensity forecasts by assimilating coastal surface currents in an idealized study. *Geophysical Research Letters*, *45*, 10,019-10,026. https://doi.org/10.1029/2018GL079677

Received 24 JUL 2018
Accepted 11 SEP 2018
Accepted article online 17 SEP 2018
Published online 28 SEP 2018

Improved Tropical Cyclone Intensity Forecasts by Assimilating Coastal Surface Currents in an Idealized Study

Yi Li[1] **and Ralf Toumi**[1]

[1] Blackett Laboratory, Department of Physics, Imperial College London, London, UK

Abstract High-frequency (HF) radars can provide high-resolution and frequent ocean surface currents observations during tropical cyclone (TC) landfall. We describe the first assimilation of such potential observations using idealized twin experiments with and without these observations. The data assimilation system consists of the Ensemble Adjustment Kalman Filter and a coupled ocean-atmosphere model. In this system, synthetic HF radar-observed coastal currents are assimilated, and the 24-, 48- and 72-hr forecast performances are examined for TCs with various intensities, sizes, and translation speeds. Assimilating coastal surface currents improves the intensity forecast. The errors of the maximum wind speed reduce by 2.7 (33%) and 1.9 m/s (60%) in the 72-hr forecast and 2.8 (40%) and 1.4 m/s (62%) in the 48-hr forecast, for Category 4 and 2 cyclones, respectively. These improvements are similar to the current operational TC forecast errors, so that assimilating HF radar observations could be a substantial benefit.

Plain Language Summary Tropical cyclones (TC) cause great loss but the forecast of the intensity has not improved significantly for a long time. High-frequency radar systems measure the coastal (up to 200 km from the coast) surface currents with high resolution, even during TC landfall. In this study, we assimilate the synthetic observations in an idealized coupled tropical cyclone forecast system. By using strongly coupled data assimilation, the ocean observations update the atmospheric state and produce significant improvements. For instance, the errors of the maximum wind speed reduce by 2.7 (33%) and 1.9 m/s (60%) in 72-hr forecast and 2.8 (40%) and 1.4 m/s (62%) in 48-hr forecast, for Category 4 and 2 cyclones, respectively. These improvements are similar to the magnitude of the current operational TC forecast error (7 and 6 m/s for 72- and 48-hr forecast), so that assimilating the radar observations could be a substantial benefit.

1. Introduction

The predictions of tropical cyclone (TC) intensity and track are of great importance. TCs affect many populous coastal regions frequently, causing casualties as well as economic and societal losses. However, the errors in the TC intensity forecasts have not decreased significantly over the past decades (e.g., Goni et al., 2017; Zhang & Weng, 2015), possibly due to error in the initial wind field (Emanuel & Zhang, 2016) or inner-core moisture (Emanuel & Zhang, 2017). The upper ocean is influenced by TCs (e.g., Price, 1981, 1983; Price et al., 1994), and the feedback affects the TC development (e.g., Bruneau et al., 2018; D'Asaro et al., 2007; Halliwell et al., 2015; Schade & Emanuel, 1999). Thus, oceanic observations have been assimilated in the TC forecast systems, including both in situ (e.g., Dong et al., 2017; Goni et al., 2017) and satellite (e.g., Halliwell, Mehari, Shay et al., 2017) observations. However, the spatial coverage of in situ observations is quite limited, especially in the coastal regions, and the satellite observations can be infrequent, impacted by clouds, and are of coarse resolution.

Here we explore the potential of high-frequency (HF) radar for tropical cyclone prediction. HF radar systems are capable of mapping coastal surface currents hourly to ranges approaching 200 km with a horizontal resolution of a few kilometers (e.g., Paduan & Washburn, 2013). The observations have been assimilated into ocean circulation models (e.g., Breivik & Sætra, 2001). It has also been shown that HF radars can produce reliable observations as tropical cyclones approach (e.g., Glenn et al., 2016; Li et al., 2017).

Data assimilation fuses the information from both observations and numerical modeling and is widely used for providing initial conditions for short-term forecasts. Coupled data assimilation systems are divided into two categories: weakly coupled and strongly coupled. The weakly coupled data assimilation updates

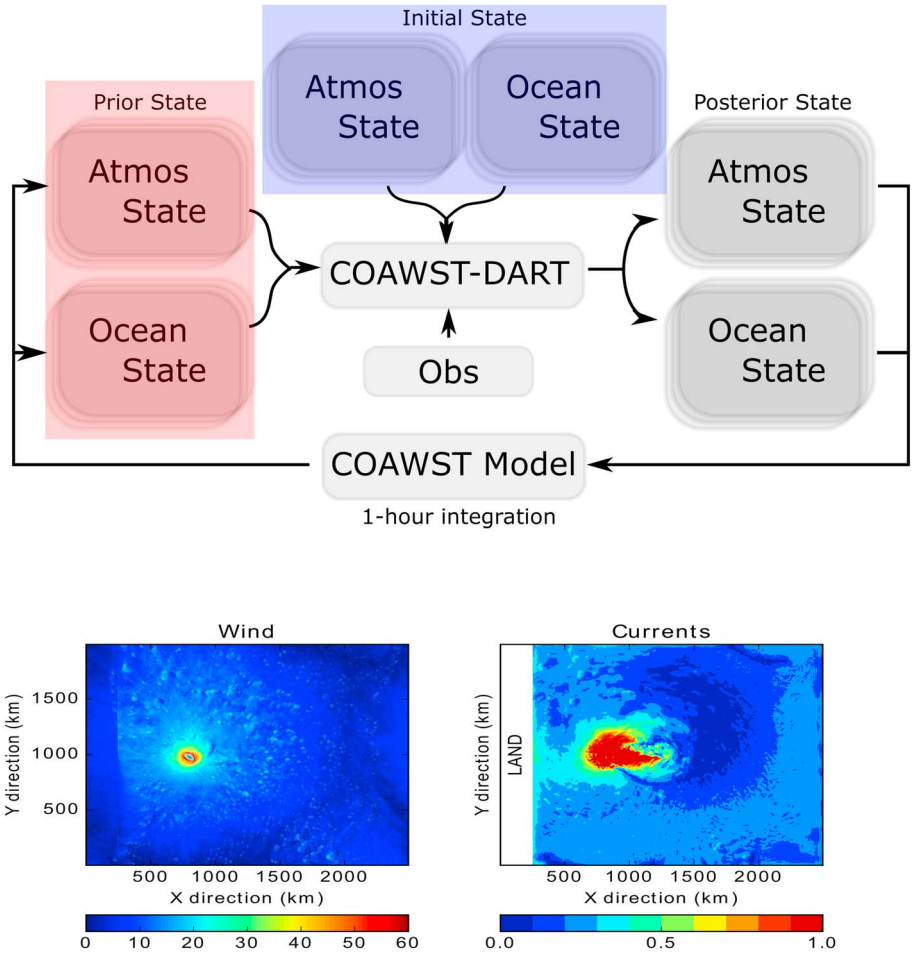

Figure 1. (upper panel) Schematic illustration of the strongly coupled DA system. At the beginning of the first cycle, the system starts from the top (blue rectangle) in which the initial state (including both oceanic (horizontal currents, temperature, salinity, and sea surface height) and atmospheric variables (horizontal wind speeds, geopotential height, temperature, surface pressure, and humidity)) is created and observed surface currents are assimilated. The posterior is used as initial condition for the 1-hr integration, whose output is used as prior state (red rectangle) in the next cycle and new observations are assimilated. This process repeats for three cycles. (lower panel) Snapshots of the surface wind speed and surface ocean currents speed at Hour T0 (i.e., 28 hr before landfall) in the TC3 case. COAWST = the Coupled-Ocean-Atmosphere-Wave-Sediment Transport modeling system; DART = Data Assimilation Research Testbed.

the states of different domains (here ocean and atmosphere) separately during the assimilation stage and integrate the numerical forecast model to exchange the information. The strongly coupled data assimilation updates the states of both domains together in the assimilation stage through the cross-domain covariance. It has been shown that strongly coupled data assimilation is superior, using either the variational (e.g., Smith et al., 2015) or the ensemble approaches (e.g., Sluka et al., 2016). Here we assimilate synthetic surface currents (observed by HF radar) in an idealized model using strongly coupled data assimilation.

2. Methods

2.1. Model Description

The strongly coupled data assimilation system (Figure 1) consists of an atmosphere-ocean coupled model and an ensemble-based data assimilation algorithm. The coupled model is a ROMS (Regional Ocean Modeling System) and WRF (Weather Research and Forecasting model) coupled model within the COAWST (Coupled-Ocean-Atmosphere-Wave-Sediment Transport modeling system [svn 830], Warner et al., 2010) framework. The domain is a 2,500-km (in x direction) × 2,000-km (in y direction) rectangle. The horizontal resolutions are set to 5 km for both ROMS and WRF. There are 31 and 27 vertical layers in WRF and ROMS, respectively. A constant Coriolis parameter of 5×10^{-5} s^{-1} is used. WRF provides a wide range of

Table 1
The Mean Translation Speed (U_h), Maximum Wind Speed (V_{max}), Minimum Pressure (P_{min}) and Azimuthal Mean Radius of the Gale-Force Wind (18 m/s, R_{18}) of the True States at the Start of the Forecast (Hour T0)

	U_h (m/s)	V_{max} (m/s)	P_{min} (hPa)	R_{18} (km)
TC1	2.8	62.7	901	160
TC2	3.7	69.5	875	220
TC3	5.3	67.2	903	215
TC4	2.8	44.1	952	100
TC5	3.7	42.0	954	100
TC6	5.3	42.6	956	120
TC7	5.3	47.2	949	80

parameterization options, and the combination is important for the success of TC simulation. The same WRF physics schemes as in Bruneau et al. (2018) are implemented.

The initial TC conditions are specified using the λ model proposed by Wang et al. (2015) and the WRF model is integrated for 3 days as spin-up without steering flow, before it is coupled with ROMS and the steering flow is added. The initial vortex is located at the center of the domain and is 1,000 km from the coastline. Seven cases are tested in this study, covering a range of sizes, intensities, and translation speeds, U_h (Table 1). In ROMS the depth is set to 1,500 m and the land is located in the west of the domain with 250-km (50 grid points) width (Figure 1). The initial subsurface temperature and salinity profiles are based on the World Ocean Atlas (WOA) climatological data set in the topical western Pacific (with the sea surface temperature (*SST*) of 28.5 °C and mixing layer depth (*MLD*) of 70 m). The initial vortices in WRF and *SST* and *MLD* in ROMS are tuned so that the TC intensities and sizes differ. We take these seven runs as the true states and calculate the errors against them.

The seven cases can be categorized into two sets. The maximum wind speed (V_{max}) of TC1, TC2, and TC3 maintains approximately 60–70 m/s (Category 4 by the Saffir Simpson scale, hereafter Cat4) during the lifetime, while TC4, TC5, TC6, and TC7 have V_{max} of 40–50 m/s (Category 2, hereafter Cat2). The minimum pressure (P_{min}) of Cat4 TCs is around 900 hPa, while Cat2 TCs is approximately 950 hPa. Generally, stronger TCs are larger. The azimuthal mean radius of the gale-force wind (18 m/s, R_{18}) in the Cat4 set is 160–220 km at T0, and TC4 and TC5 are 100 km, while TC6 is 120 km. TC7 is particularly small and its R_{18} is 80 km at *T*0. The forecasts start at Hour T0 (1 day after the spin-up), and the cyclones make landfall at Hour $T+75$, $T+52$, and $T+28$ with translation speeds of 2.8, 3.7, and 5.3 m/s, respectively. During the period of data assimilation (Hour *T*-3 to *T*0), the TC centers are about 600–800 km from the coastline. We study Hour *T*0 to $T+24$, *T*0 to $T+48$, and *T*0 to $T+72$ as the period of forecast.

2.2. Data Assimilation

The data assimilation algorithm used in this study is a variety of ensemble Kalman filter, the Ensemble Adjustment Kalman Filter (EAKF) algorithm (Anderson, 2001), provided by the Data Assimilation Research Testbed (DART) package (Version Lanai, https://www.image.ucar.edu/DAReS/DART/Lanai/index.html; Anderson et al., 2009).

OSSEs are often used to estimate the value of potential observations or the benefit of data assimilation (e.g., Halliwell, Mehari, Shay et al., 2017; Sluka et al., 2016). OSSEs are based on twin experiments where synthetic observations are assimilated in different ways. Here we design the twin experiments that one ensemble assimilates the synthetic ocean currents (hereafter DA) and the other does not (hereafter NoDA) for each case.

The initial ensembles play an important role in the success of a data assimilation system. In this study we generate the ensembles by perturbing the model *truth*. For all the cases, the coupled models are perturbed at Hour *T*-12, using the CV3 background error covariance option (Barker et al., 2004) in the WRF three-dimensional variational data assimilation (3D-Var) package. Then the perturbed ensembles are integrated with the ROMS model for 9 hr to develop realistic, physically balanced states, which are used as the initial ensembles for DA and initial conditions for the NoDA runs (Zhang et al., 2006, 2009).

In all the cases, the observations are created from the corresponding model *truth* by extracting the top layer (about 28 cm) ocean currents located 5 km to 200 km (1 to 40 grid points) away from the coastline with 5-km

spatial resolution and hourly temporal resolution, similar to what HF radar systems can achieve. The data within 600 km from the south and north boundaries are discarded. The data assimilation systems are sensitive to several parameters (e.g., Houtekamer & Zhang, 2016), including the localization schemes, ensemble sizes, the assumptions regarding the observation errors. In this study, we assume that the observations have independent, Gaussian random errors of 0 mean and variance of 10 cm/s (Paduan & Washburn, 2013). Sensitivity tests (shown in the supporting information) confirm that 10 cm/s is an optimal value. In real cases the currents are influenced by bathymetry and background flow and more tests (e.g., reforecast experiments) are needed. The observations are assimilated using EAKF provided by DART, which supports many geophysical models including ROMS (Li & Toumi, 2017) and WRF (Anderson et al., 2009). In the strongly coupled data assimilation system, the error covariance matrix is calculated using the variables of both models. Forty ensemble members are used in this study, and the oceanic variables included are horizontal currents, temperature, salinity, and sea surface height, and the atmospheric variables are horizontal wind speeds, geopotential height, temperature, surface pressure, and humidity. The localization technique is needed in the ensemble data assimilation with limited ensemble size to reduce the spurious covariance between distant points (e.g., Houtekamer & Mitchell, 2001; Miyoshi et al., 2014). The Gaspari-Cohn localization function (Gaspari & Cohn, 1999) is used with the half-width radius of 700 km. The horizontal localization scale is selected after several sensitivity experiments (shown in the supporting information). Successive covariance localization methods (e.g., Zhang et al., 2009) have shown advantages to any single localization in WRF simulations and may provide potential improvements, but in this proof-of-concept study, only single localization is used. Vertically, the localization is five layers for WRF and no vertical localization is used for ROMS. The correlations between atmospheric vertical profiles (temperature, humidity, and wind) with the local surface ocean currents are computed (shown in the supporting information) and the correlations are high below 940 hPa (the bottom five layers), thus the vertical localization scale of 5 is chosen (Fowler & Lawless, 2016; Smith et al., 2017). In this study, we perform 24-, 48- and 72-hr forecast experiments. In each of the experiments, three cycles of assimilation with 1-hr window are performed and then the forecasts are made.

2.3. Forecast Evaluation

Conventionally, the maximum wind speed (V_{max}) is used to estimate the destructiveness of TCs. However, V_{max} does not reflect the size and structure of TCs and therefore can be misleading for some large cyclones. For example, Hurricane Sandy (2012) caused great damage in the Caribbean islands and the United States although its peak V_{max} was just 100 kt (51 m/s, Category 3). Thus, other metrics are needed to approximate the damage potential. Studies have shown that the integrated power dissipation (*IPD*; Emanuel, 2005) is superior to V_{max} in describing the damage potential (e.g., Wang & Toumi, 2016). In this study, V_{max}, the minimum pressure (P_{min}), and *IPD* are used as metrics of TC intensity. The metrics of each ensemble member are calculated separately and the error is the difference between the *truth* and the ensemble mean.

3. Results

3.1. The *Truth* and Synthetic Observations

As described above, seven cases are created as the true states, with varying intensities, sizes, and translation speeds (Table 1). In the Cat4 set (TC1, TC2, and TC3), the maximum wind speed decreases to 58–63 m/s as the cyclones move toward the land. In the Cat2 set (TC4, TC5, TC6, and TC7), the V_{max} is 43–50 m/s when the cyclones make landfall. The R_{18} in the Cat4 set increases to 180–220 km at the landfall and TC4 and TC5 grow to 150–160 km while TC6 remains 120 km. TC7 decreases to 60 km at landfall. Stronger TCs are also more destructive. The *IPD* at landfall is 11–12 TW in the Cat4 set, while TC4 and TC5 have *IPD* of 6–7 TW and TC6 and TC7 are even weaker (2–3 TW). We use the currents generated from these cases as the synthetic observations and assimilate them.

3.2. The Data Assimilation and Forecast

The influence of TCs on coastal currents is well known (e.g., Keen & Glenn, 1999), but the quantitative relationship between coastal currents and TC intensity and location is complex. In the strongly coupled data assimilation, the observation in the ocean affects the atmosphere directly via the cross covariance. Therefore, the high correlations between the oceanic and atmospheric states are desired for a successful assimilation. For a strongly coupled phenomenon such as a TC, the oceanic and atmospheric states are highly correlated and the surface coastal currents change significantly ahead of the TC center (Figure 1; e.g., Bruneau et al., 2018; Glenn et al., 2016). Here we take the DA run of TC3 as an example. Figure 2 shows the ensemble correlation of the coastal surface currents with the tracks and *IPD* of the cyclone. The correlations are shown instead

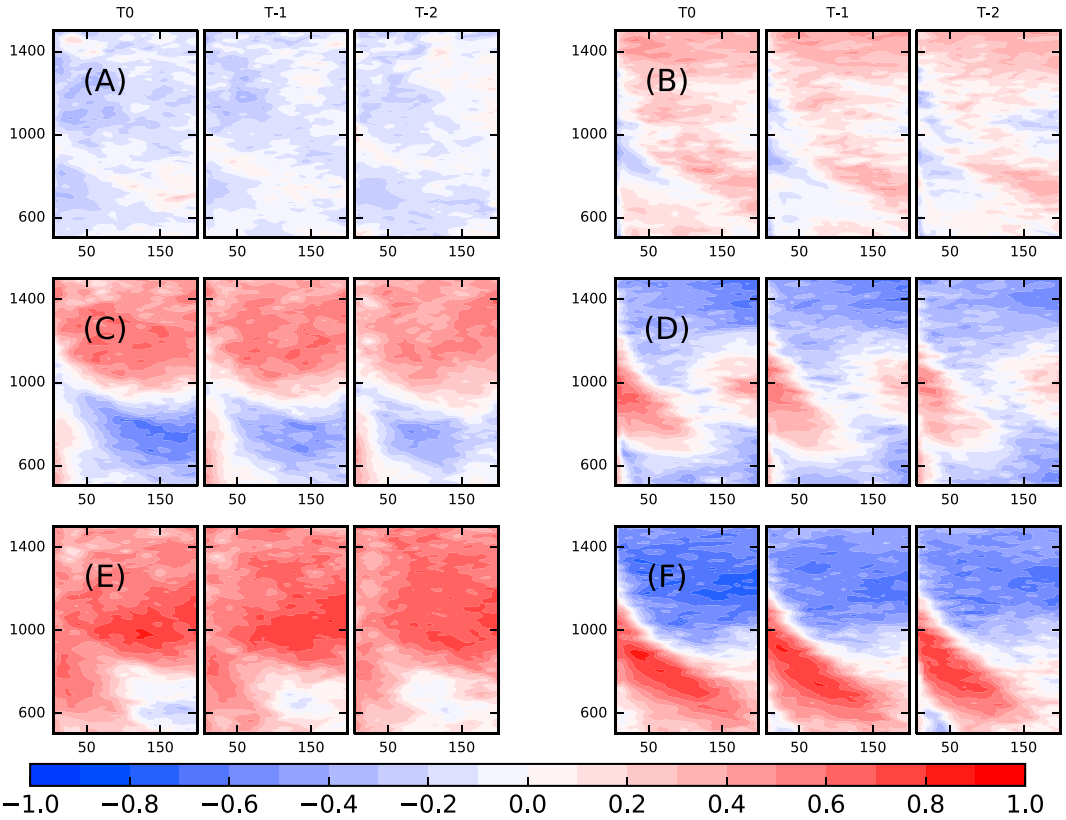

Figure 2. The spatial distribution of the error correlations between the coastal (left panel) *u*, (right panel) *v* currents in ROMS with (a, b) *IPD* and (c, d) longitude and (e, f) latitude of the TC center. The correlations are calculated from the posterior states of the DA ensemble in the TC3 case during the period of data assimilation. The region is from 5 to 200 km from coast in the *x* direction and along the coast from 500 to 1,500 km in the *y* direction. The TC is moving to the left (westward). Each box in each subplot represent a time point (from right to left, Hour T-2 to T0). The *x* axis in each box is distance (km) the from 5 to 200 km from the coast. The *y* axis is the distance (km) in the *y* direction.

of the covariances because the covariances of the coupled state vector are dominated by the variables with large variances. At the beginning of the data assimilation (Hour *T*-2), the TC center is 30-hr (approximately 600 km) away from the coastline, the correlations between the currents and TC location is about 0.5 and 0.2–0.3 between currents and *IPD*. As the cyclone moves toward the coastline, the correlations between currents and *IPD* increase to 0.3–0.4 two hours later. Other cases depict similar correlation pattern but in the Cat2 set the values are smaller (figure not shown).

Twenty-four-, 48-, and 72-hr forecasts are conducted in this study, for the cyclones with different translation speeds (e.g., 24-, 48-, and 72-hr forecasts for TC1 and TC4 with translation speed of 2.8 m/s and 24-hr forecasts for TC3 and TC6). Assimilating the synthetic ocean currents observations improve the TC forecasts in all cases (Figure 3). The benefit is higher for the stronger cyclones and increases with the lead time for each case, the relative error displays similar trends (figure not shown). For the 72-hr forecast, the error of V_{max} reduces by 2.7 m/s (33%) for TC1 (Category 4) and 1.9 m/s (60%) for TC4 (Category 2). For the 48-hr forecast, the average improvement is 2.8 m/s (40%) for the stronger cyclones and 1.4 m/s (62%) for the weaker ones. At the lead time of 24 hr, the improvements are around 1 m/s (25%) for the TCs that move slower than 4 m/s but is as high as 3.7 m/s (50%) for the fast one (TC3). However, the improvement is marginal for TC7, which is much smaller than other cyclones.

Higher forecast skill is also seen for the minimum pressure. The error decreases by 7 hPa (over 50%) for the 72-hr forecast in the Category 4 case (TC1). When the cyclone is weaker (TC4), the 72-hr forecast improves by 4 hPa (45%). The error reduces by 3–6 hPa for the 48-hr forecast. As for the 24-hr forecast, the error falls by over 3 hPa, on average. Similar with the V_{max}, the improvement for the small and weak case (TC7) is insignificant.

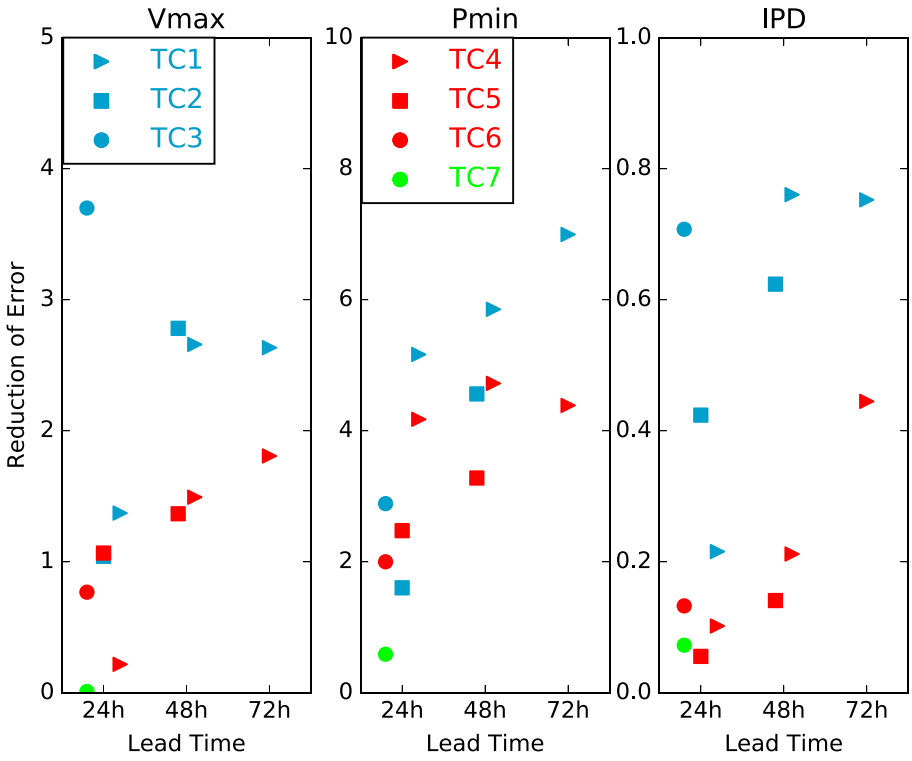

Figure 3. The difference (NoDA − DA) of errors in V_{max}, P_{min}, and *IPD*. The units are m/s, hPa, and TW, respectively. IPD = integrated power dissipation.

IPD is not currently an operational verifiable error metric but has shown great potential on describing the destructiveness (e.g., Wang & Toumi, 2016). Here assimilating the synthetic ocean currents observations reduces the error of *IPD* dramatically, especially for the stronger cases, in which the improvement is as high as over 0.6 TW for the 48- and 72-hr forecasts. The 24-hr forecast for the Cat4 cases is also promising, but the results diverge and more benefit is shown for the fast-moving cyclones. The error for TC3, with translation speed of 5.3 m/s, reduces by 0.7 TW (50%), and the reduction for TC2 (3.7 m/s) and TC1 (2.8 m/s) is 0.4 and 0.2 TW, respectively. For the Cat2 set, the error of the 72-hr forecast reduces by 0.4 TW (50%), but the benefit for the 24- and 48-hr forecast is less than 0.2 TW (30%).

4. Discussion and Conclusion

It has been well known that the coastal surface currents respond to the approaching cyclones, and this can be monitored by HF radars (e.g., Bruneau et al., 2018; Glenn et al., 2016). However, this potentially useful observation is not assimilated in TC forecast systems. In this study we develop a strongly coupled data assimilation system using the EAKF and the COAWST and assimilate synthetic surface coastal currents in an idealized OSSE. The effects are evaluated in both weak (Category 2) and strong (Category 4) TC cases, with various sizes and translation speeds. By performing strongly coupled data assimilation, the ocean observations update the atmosphere state directly via the cross-covariance matrix and lead to substantial benefit for TC forecasts.

Higher forecast skills are shown for almost all the cases, with different intensities, sizes, and translation speeds. For instance, the error of maximum wind speed (V_{max}) reduces by 2.7 m/s (33%) for the 72-hr forecast of a Category 4 TC, the 48-hr forecast is also improved significantly (2.8 m/s, 40%). For the weaker cyclones (Category 2), the error also decreases by 1.4–1.9 m/s (60%). These reductions are of similar order with the current real-time forecast of 7, 6, and 5 m/s for the 72-, 48-, and 24-hr (e.g., Goni et al., 2017). These improvements are achieved mainly by adjusting the initial atmospheric conditions because of the strong correlation between the coastal currents and the TC wind field (Figure 2). In the case of weakly coupled data assimilation, where assimilating ocean variables do not update the atmospheric states, the forecast skill is worse than the strongly coupled and control cases (shown in the supporting information). When other traditional observations, especially the atmospheric variables, are also assimilated, the benefit of assimilating ocean currents would be

expected to be smaller. However, weather radar or satellite data do not give direct or frequent boundary layer state information, which the HF radar can potentially provide.

Assimilating the synthetic observations also improves the forecast of TC tracks by around 10% but it is noteworthy that in these idealized experiments, the errors of TC tracks (order of 10 km) are much lower than the real-time forecast errors (order of 50 km; e.g., Yamaguchi et al., 2017). However, the benefit is marginal for a weak and small cyclone (with R_{18} of 60–80 km) although the track forecast improves in this case. This is because the assimilation of coastal currents adjusts the large-scale circulation and can improve the structure of the large TC and the steering flow. Therefore, the assimilation works better for the intensity of large TCs and tracks of small ones. The typical value of R_{18} in real cases is 150–250 km (e.g., Chan & Chan, 2015; Sampson et al., 2017), similar with the larger cases in this study, and thus, we anticipate that the actual benefit in practice would be substantial.

HF radars can produce accurate measurements during TC landfall while much of other ocean observing systems (e.g., Argo floats and gliders) are usually unavailable or impacted. Halliwell, Mehari, Shay, et al. (2017) and Halliwell, Mehari, Le Henaff, et al. (2017) pointed out that assimilating standard ocean observations (e.g., sea surface temperature and sea level anomaly) produced a better ocean state and could potentially improve TC forecast but the actual benefit was not demonstrated. In a real case study of Hurricane Gonzalo (2014, Category 4 with V_{max} over 60 m/s), Dong et al. (2017) found that underwater glider observations had no effect on the TC forecast. The potential benefit of HF radar is demonstrated here. However, more studies are needed to estimate the influence of other factors in real cases and settings, including the combination of different observations, background ocean currents, and bathymetry.

Ensemble data assimilation can generate the cross-domain background error covariance automatically, and the implementation of strongly coupled data assimilation is feasible. In addition, unlike other observations such as airborne profilers, which need to be deployed, the typical HF radar network is already immediately available to gather observations. This work suggests potential benefits of assimilating coastal current observations in coupled TC forecast systems.

Acknowledgments
This study is sponsored by the Chinese Scholarship Council (CSC)-Imperial College London scholarship and the Climate Science Service Partnership China (UK Met Office/Newton Fund). The model scripts used in this study are described in section 2. We would like to thank the two anonymous reviewers for their insightful comments and suggestions.

References

Anderson, J. L. (2001). An ensemble adjustment Kalman filter for data assimilation. *Monthly Weather Review*, *129*, 2884–2903. https://doi.org/10.1175/1520-0493(2001)129<2884:AEAKFF>2.0.CO;2

Anderson, J., Hoar, T., Raeder, K., Liu, H., Collins, N., Torn, R., et al. (2009). The data assimilation research testbed: A community facility. *Bulletin of the American Meteorological Society*, *90*(9), 1283–1296. https://doi.org/10.1175/2009BAMS2618.1

Barker, D. M., Huang, W., Guo, Y.-R., Bourgeois, A. J., Xiao, Q. N., Barker, D. M., et al. (2004). A three-dimensional variational data assimilation system for MM5: Implementation and initial results. *Monthly Weather Review*, *4*, 897–914. https://doi.org/10.1175/1520-0493(2004)132<0897:ATVDAS>2.0.CO;2

Breivik, Ø., & Sætra, Ø. (2001). Real time assimilation of HF radar currents into a coastal ocean model. *Journal of Marine Systems*, *28*(3-4), 161–182. https://doi.org/10.1016/S0924-7963(01)00002-1

Bruneau, N., Toumi, R., & Wang, S. (2018). Impact of wave whitecapping on land falling tropical cyclones. *Scientific Reports*, *8*(1), 652. https://doi.org/10.1038/s41598-017-19012-3

Chan, K. T., & Chan, J. C. (2015). Global climatology of tropical cyclone size as inferred from QuikSCAT data. *International Journal of Climatology*, *35*(15), 4843–4848. https://doi.org/10.1002/joc.4307

D'Asaro, E. A., Sanford, T. B., Niiler, P. P., & Terrill, E. J. (2007). Cold wake of Hurricane Frances. *Geophysical Research Letters*, *34*, L15609. https://doi.org/10.1029/2007GL030160

Dong, J., Domingues, R., Goni, G., Halliwell, G., Kim, H.-S., Lee, S.-K., et al. (2017). Impact of assimilating underwater glider data on Hurricane Gonzalo (2014) forecasts. *Weather and Forecasting*, *32*(3), 1143–1159. https://doi.org/10.1175/WAF-D-16-0182.1

Emanuel, K. (2005). Increasing destructiveness of tropical cyclones over the past 30 years. *Nature*, *436*(7051), 686–688. https://doi.org/10.1038/nature03906

Emanuel, K., & Zhang, F. (2016). On the predictability and error sources of tropical cyclone intensity forecasts. *Journal of the Atmospheric Sciences*, *73*(9), 3739–3747. https://doi.org/10.1175/JAS-D-16-0100.1

Emanuel, K., & Zhang, F. (2017). The role of inner-core moisture in tropical cyclone predictability and practical forecast skill. *Journal of the Atmospheric Sciences*, *74*(7), 2315–2324. https://doi.org/10.1175/JAS-D-17-0008.1

Fowler, A. M., & Lawless, A. S. (2016). An idealized study of coupled atmosphere-ocean 4D-Var in the presence of model error. *Monthly Weather Review*, *144*(10), 4007–4030. https://doi.org/10.1175/MWR-D-15-0420.1

Gaspari, G., & Cohn, S. E. (1999). Construction of correlation functions in two and three dimensions. *Quarterly Journal of the Royal Meteorological Society*, *125*(554), 723–757. https://doi.org/10.1002/qj.49712555417

Glenn, S. M., Miles, T. N., Seroka, G. N., Xu, Y., Forney, R. K., Yu, F., et al. (2016). Stratified coastal ocean interactions with tropical cyclones May 2015. *Nature Communications*, *7*(10), 887. https://doi.org/10.1038/ncomms10887

Goni, G., Todd, R., Jayne, S., Halliwell, G., Glenn, S., Dong, J., et al. (2017). Autonomous and Lagrangian ocean observations for Atlantic tropical cyclone studies and forecasts. *Oceanography*, *30*(2), 92–103. https://doi.org/10.5670/oceanog.2017.227

Halliwell, G. R., Gopalakrishnan, S., Marks, F., & Willey, D. (2015). Idealized study of ocean impacts on tropical cyclone intensity forecasts. *Monthly Weather Review*, *143*(4), 1142–1165. https://doi.org/10.1175/MWR-D-14-00022.1

Halliwell, G. R., Mehari, M. F., Le Hënaff, M., Kourafalou, V. H., Androulidakis, I. S., Kang, H. S., et al. (2017). North Atlantic Ocean OSSE system: Evaluation of operational ocean observing system components and supplemental seasonal observations for

potentially improving tropical cyclone prediction in coupled systems. *Journal of Operational Oceanography*, *10*(2), 154–175. https://doi.org/10.1080/1755876X.2017.1322770

Halliwell, G. R., Mehari, M., Shay, L. K., Kourafalou, V. H., Kang, H., Kim, H.-S., et al. (2017). OSSE quantitative assessment of rapid-response prestorm ocean surveys to improve coupled tropical cyclone prediction. *Journal of Geophysical Research: Oceans*, *122*, 5729–5748. https://doi.org/10.1002/2017JC012760

Houtekamer, P. L., & Mitchell, H. L. (2001). A sequential ensemble Kalman filter for atmospheric data assimilation. *Monthly Weather Review*, *129*(1), 123–137. https://doi.org/10.1175/1520-0493(2001)129<0123:ASEKFF>2.0.CO;2

Houtekamer, P. L., & Zhang, F. (2016). Review of the ensemble Kalman filter for atmospheric data assimilation. *Monthly Weather Review*, *144*(12), 4489–4532. https://doi.org/10.1175/MWR-D-15-0440.1

Keen, T. R., & Glenn, S. M. (1999). Shallow water currents during Hurricane Andrew. *Journal of Geophysical Research*, *104*(C10), 23,443–23,458. https://doi.org/10.1029/1999JC900180

Li, Y., & Toumi, R. (2017). A balanced Kalman filter ocean data assimilation system with application to the South Australian Sea. *Ocean Modelling*, *116*, 159–172. https://doi.org/10.1016/j.ocemod.2017.06.007

Li, C., Wang, H., Gao, J., Li, H., Wang, G., Pan, S., et al. (2017). Data analysis of the high frequency surface wave radar during Typhoon Chan-hom. *IOP Conference Series: Earth and Environmental Science*, *52*(1), 012019. https://doi.org/10.1088/1742-6596/52/1/012019

Miyoshi, T., Kondo, K., & Imamura, T. (2014). The 10,240-member ensemble Kalman filtering with an intermediate AGCM. *Geophysical Research Letters*, *41*, 5264–5271. https://doi.org/10.1002/2014GL060863

Paduan, J. D., & Washburn, L. (2013). High-frequency radar observations of ocean surface currents. *Annual Review of Marine Science*, *5*(1), 115–136. https://doi.org/10.1146/annurev-marine-121211-172315

Price, J. F. (1981). Upper ocean response to a hurricane. *Journal of Physical Oceanography*, *11*, 153–175. https://doi.org/10.1175/1520-0485(1981)011<0153:UORTAH>2.0.CO;2

Price, J. F. (1983). Internal wave wake of a moving storm. Part I. Scales, energy budget and observations. *Journal of Physical Oceanography*, *13*, 949–965. https://doi.org/10.1175/1520-0485(1983)013<0949:IWWOAM>2.0.CO;2

Price, J. F., Sanford, T. B., & Forristall, G. Z. (1994). Forced stage response to a moving hurricane. *Journal of Physical Oceanography*, *24*(2), 233–260. https://doi.org/10.1175/1520-0485(1994)024<0233:FSRTAM>2.0.CO;2

Sampson, C. R., Fukada, E. M., Knaff, J. A., Strahl, B. R., Brennan, M. J., & Marchok, T. (2017). Tropical cyclone gale wind radii estimates for the western North Pacific. *Weather and Forecasting*, *32*(3), 1029–1040. https://doi.org/10.1175/WAF-D-16-0196.1

Schade, L. R., & Emanuel, K. A. (1999). The ocean's effect on the intensity of tropical cyclones: Results from a simple coupled atmosphere-ocean model. *Journal of the Atmospheric Sciences*, *56*(4), 642–651. https://doi.org/10.1175/1520-0469(1999)056<0642:TOSEOT>2.0.CO;2

Sluka, T. C., Penny, S. G., Kalnay, E., & Miyoshi, T. (2016). Assimilating atmospheric observations into the ocean using strongly coupled ensemble data assimilation. *Geophysical Research Letters*, *43*, 752–759. https://doi.org/10.1002/2015GL067238

Smith, P. J., Fowler, A. M., & Lawless, A. S. (2015). Exploring strategies for coupled 4D-Var data assimilation using an idealised atmosphere-ocean model, Tellus. *Series A: Dynamic Meteorology and Oceanography*, *67*(1), 1–25. https://doi.org/10.3402/tellusa.v67.27025

Smith, P. J., Lawless, A. S., & Nichols, N. K. (2017). Estimating forecast error covariances for strongly coupled atmosphere-ocean 4D-Var data assimilation. *Monthly Weather Review*, *145*(10), 4011–4035. https://doi.org/10.1175/MWR-D-16-0284.1

Wang, S., & Toumi, R. (2016). On the relationship between hurricane cost and the integrated wind profile. *Environmental Research Letters*, *11*(114005). https://doi.org/10.1088/1748-9326/11/11/114005

Wang, S., Toumi, R., Czaja, A., & Kan, A. V. (2015). An analytic model of tropical cyclone wind profiles. *Quarterly Journal of the Royal Meteorological Society*, *141*(693), 3018–3029. https://doi.org/10.1002/qj.2586

Warner, J. C., Armstrong, B., He, R., & Zambon, J. B. (2010). Development of a Coupled Ocean-Atmosphere-Wave-Sediment Transport (COAWST) modeling system. *Ocean Modelling*, *35*(3), 230–244. https://doi.org/10.1016/j.ocemod.2010.07.010

Yamaguchi, M., Ishida, J., Sato, H., & Nakagawa, M. (2017). WGNE intercomparison of tropical cyclone forecasts by operational NWP models: A quarter century and beyond. *Bulletin of the American Meteorological Society*, *98*(11), 2337–2349. https://doi.org/10.1175/BAMS-D-16-0133.1

Zhang, F., Meng, Z., & Aksoy, A. (2006). Tests of an ensemble Kalman filter for mesoscale and regional-scale data assimilation. Part I: Perfect model experiments. *Monthly Weather Review*, *134*(2), 722–736. https://doi.org/10.1175/MWR3101.1

Zhang, F., & Weng, Y. (2015). Predicting hurricane intensity and associated hazards: A five-year real-time forecast experiment with assimilation of airborne Doppler radar observations. *Bulletin of the American Meteorological Society*, *96*(1), 25–33. https://doi.org/10.1175/BAMS-D-13-00231.1

Zhang, F., Weng, Y., Sippel, J. A., Meng, Z., & Bishop, C. H. (2009). Cloud-resolving hurricane initialization and prediction through assimilation of Doppler radar observations with an ensemble Kalman filter. *Monthly Weather Review*, *137*(7), 2105–2125. https://doi.org/10.1175/2009MWR2645.1